

Patched-FLANNEL: COVID-19 X-ray Image Classification

https://mediaspace.illinois.edu/media/t/1_atvzrp1d

Maneesh Kumar
Singh

University of Illinois at
Urbana-Champaign

mksingh4@illinois.edu

Raman
Walwyn-Venugopal

University of Illinois at
Urbana-Champaign

rsw2@illinois.edu

Satish Reddy Asi

University of Illinois at
Urbana-Champaign

sasi2@illinois.edu

Srikanth Bharadwaz
Samudrala

University of Illinois at
Urbana-Champaign

sbs7@illinois.edu

ABSTRACT

Objective: Detecting COVID-19 using Chest X-Ray (CXR) images is becoming increasingly popular in deep learning research. When training deep neural networks, large and balanced datasets are preferred. However, since COVID-19 is new, there are a limited number of CXR images available which results in a challenge for training deep neural networks. Existing research has shown different approaches to address this imbalanced data issue. Two notable studies are FLANNEL (Focal Loss bAsed Neural Network EnsembLe) model and a patch-based classifier that works on segmented versions of the lung contours. We propose merging these two concepts together to improve performance of detecting COVID-19 in CXR images.

Materials and Methods: As a pre-processing step, use a segmentation network to create a masked CXR images that only displays the lung areas. Replace base models in FLANNEL with patch-based classifiers that take masked image as input. The patch-based classifiers are used for the ensemble.

Results: We are able to reproduce FLANNEL with updated datasets. We created a segmentation network that can produce masks of the lung contours for CXR images and successfully used it to generate masked CXR images of the updated FLANNEL datasets. The FLANNEL base models were successfully updated to be patch-based classifiers. The overall modifications resulted in similar performance of the original FLANNEL architecture, where some metrics improved while others decreased.

Discussion: We saw improvement in metrics when training the base models and FLANNEL ensemble over updated dataset. Since no parameters were changed, we suspect that this is due to the large increase of COVID-19 images in the dataset compared to when the FLANNEL paper was written. When training the patch-based models, we noticed that some patch-based models slightly improved in performance while others slightly decreased but there were no major differences.

Conclusion: With the Patched FLANNEL barely outperforming FLANNEL in certain metrics, we believe there is merit to conduct further research to determine if more improvements can be made. Potential areas that can be further developed are but not limited to; segmentation, data augmentation, changing number of patches, changing size

of patch and more. However, it should be noted that the largest improvement in overall metrics when compared to the original FLANNEL with the old dataset is due to the updated dataset having a large increase in COVID-19 images. This highlights how crucial getting quality data is to improve performance on models.

1. INTRODUCTION

Coronavirus disease 2019 (COVID-19) is a contagious disease caused by severe acute respiratory syndrome Coronavirus 2 (SARS-CoV-2). It has spread worldwide leading to an ongoing pandemic. This pandemic has ravaged the world on an unprecedented scale. By April 2021, 141 million people have been infected and there are over 3 million deaths [14]. Chest X-Ray (CXR) is one of the important, non-invasive clinical diagnosis tools that helps to detect COVID-19 and other pneumonia for affected patients.

Using deep learning for X-ray classification is an ongoing research area and recently there have been promising models proposed for COVID-19 classification. The problem that all of these models face is an imbalanced dataset due to the limited number of COVID CXR images available.

FLANNEL is a COVID-19 CXR classification model proposed by Zhi Qiao et al. [10] that has been shown to accurately detect COVID-19 even when trained with only 100 available COVID-19 x-ray images. There are two core components for the FLANNEL architecture, the first is that it uses an ensemble [4] of five independent base models that predict the classification of the CXR. Each of the predictions are then passed through another neural weight network to determine the final prediction classification. The goal of the ensemble is to increase the robustness and accuracy of the network since each base model should capture patterns in the images independently [11]. The second core component for the FLANNEL is its use of the special Focal Loss [7] function, a modification of the standard cross-entropy loss that places a focus on the imbalance negatives by applying down-weights to well-classified examples. Focal Loss has been known to improve performance for imbalanced datasets.

Park et al. [9] has also created a deep learning model that has been proven to be effective on detecting COVID-19 when trained with limited datasets. The approach taken was to first detect lung contours of the CXR and perform segmentation. The motivation for performing segmentation first is that the patch based model focuses on the lung area since it's the primary region of interest used to perform analy-

sis. In general, standard biomarkers [9] from CXR images analyzed are the following

1. Lung Morphology
2. Mean Lung Intensity
3. Standard Deviation of Lung Intensity
4. Cardiothoracic Ratio (CTR)

Thus it could be observed that most of the initial diagnosis is carried out from CXR images by concentrating on the lung area. We also find this strategy also makes the model less susceptible to noise happening outside the lung region. After the lungs have been segmented, patch-based classification is performed. Patch-based classification involves selecting random crops or patches across the image for a set number of times and then performing classification on each patch. Afterwards, the final prediction of the image is made by majority voting based on the prediction of each patch. The advantage of using a patch-based approach for classification is that since the classification is on a smaller part of the image, the network has a higher chance of recognizing “local” patterns, unfortunately the disadvantage of using a patch-based approach is more likely for the image to not recognize “global” patterns throughout the whole image. Based on the conclusion provided in the patch based paper [9] by Park et al., it is clear that the patch-based classification outperformed the models that used the whole image for a limited train set data. As we have an imbalanced dataset with limited COVID 19 CXR images, we were optimistic that utilizing patch-based classification models for the FLANNEL ensemble with the combination of focal loss optimization would result in a performance improvement.

Our goal was to take the novel ideas of each approach listed above with the goal of improving performance. To accomplish this we made modifications to the existing FLANNEL architecture by first pre-processing the CXR images by performing segmentation of the lung contours. Afterwards, we updated the independent base models in the ensemble to be patch-based classifiers. We call this new architecture **Patched FLANNEL**. The network structure is shown in Figure 1 and similar to FLANNEL consists of two-stage approach.

1.1 Related Work

Here we discuss some of the related works that are being carried out in this area on using deep learning techniques to detect COVID-19. Most of these works either used CXR or CT scans for patients to detect COVID-19. Our current research also falls in the same lines to accurately classify the patients CXR images to COVID-19 class or non COVID-19 classes.

1.1.1 AI-COVID

X. Bai and Wang [1] were able to create an AI system that could differentiate COVID-19 and other pneumonia using a chest CT scan. They approached this as a classification problem and used the EfficientNet B4 architecture which was a CNN based network. They were able to achieve results of 96% accuracy, 95% sensitivity, 96% specificity, and an area under receiver operating characteristic curve of 0.95 and an area under the precision recall curve of 0.90. When compared with radiologists on the same test dataset, the AI

system performed better. This study concluded that the AI can support radiologists in detection of COVID-19 in Chest CT images.

1.1.2 COVID-Net

Wang et al. are able to create COVID-Net [13] architecture by considering COVIDx dataset which contains 13,975 CXR images for training and experiments. COVID-Net architecture makes heavy use of a lightweight residual ‘projection expansion projection extension’ (PPEX) design pattern that contains multiple levels of convolution layers with fully connected layers and a softmax at the end. COVID-Net achieved higher test accuracy than other architectures such as VGG-19 and ResNet-50.

1.1.3 Focal loss for dense object detection

Lin et al. propose Focal loss [7], a modification to the standard cross entropy criterion that focuses weights for loss on hard examples versus well classified examples. This is accomplished by adding a factor $(1 - p_t)^\gamma$ to the standard cross entropy criterion where setting $\gamma > 0$ reduces the relative loss for well-classified examples ($p_t > .5$). This results in achieving higher accuracy than using the standard cross entropy loss and surpassed speed and accuracy when compared with state of the art two stage detectors; Faster R CNN Variants.

1.1.4 Ensemble Models

FLANNEL model applies ensemble approach to combine multiple base learners to get classification from each model. As shown by Larse Kai Hansen and Peter Salamon [4] compared to individual model, a better classification can be achieved by training an ensemble of neural networks on same data and then using a consensus scheme to decide the collective classification by vote.

Modular ensemble models have also been shown to perform better and reduce training time in several researches [11]. It has been also shown to reduce model complexity and making the overall system easier to understand.

1.1.5 Noise-robust segmentation of COVID-19 from CT images

This is a CNN model [12] developed to be effective with detection of COVID-19 lesions from CT images that have a lot of noise. This paper discusses how Wang et al developed a novel noise-robust learning framework based on self-ensembling of CNNs. To better deal with the complex lesions, a novel COVID-19 Pneumonia Lesion segmentation network (COPLE-Net) was proposed that uses a combination of max-pooling and average pooling to reduce information loss during downsampling, and employs bridge layers to alleviate the semantic gap between features in the encoder and decoder. Experimental results with CT images of 558 COVID-19 patients showed the effectiveness of the noise-robust Dice loss function, COPLE-Net and adaptive self-ensembling in learning from noisy labels for COVID-19 pneumonia lesion segmentation. To make the training process robust against noisy labels, a novel noise-robust Dice loss function was proposed and integrated into a self-ensembling framework, where an adaptive teacher and an adaptive student are introduced to further improve the performance in dealing with noisy labels.

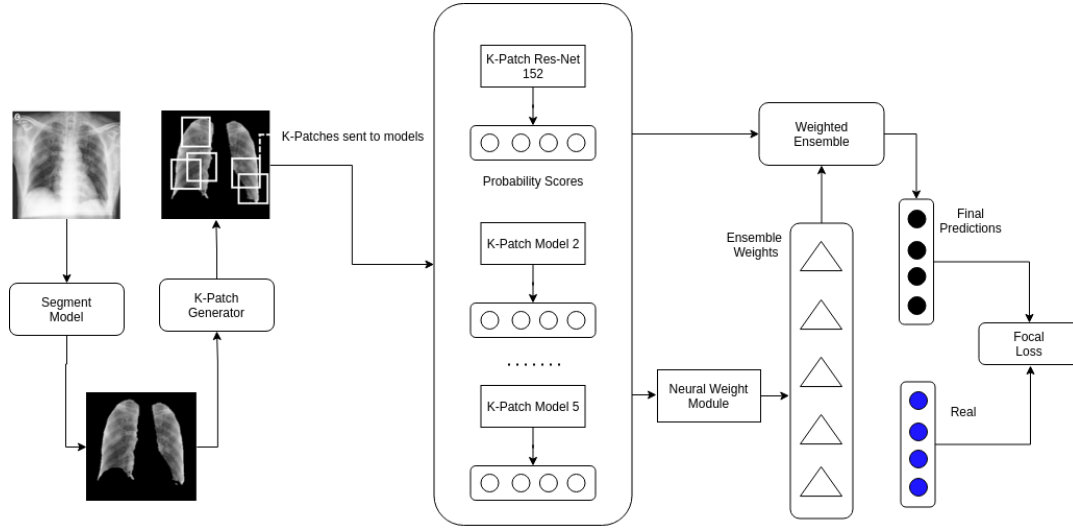


Figure 1: FLANNEL Improvement

1.1.6 Automatic Detection of COVID-19 using CXR images

A Narin et al. trained 5 different models to effectively classify the CXR images into 3 different binary classes [8], such as COVID19 vs Normal, COVID19 vs Pneumonia Bacteria and COVID19 vs Pneumonia Viral. They have used datasets from github repository shared by Dr. Joseph Cohen which contains CXR and CT images with ARDS, COVID-19, MERS, pneumonia and SARS. Health Chest X-rays are taken from “ChesX-ray8” dataset and also collected bacterial, pneumonia viral CXRs from Kaggle repository. They were able to achieve accuracies of 96.1%, 99.5% and 99.7% for the three different binary classifications, COVID19 vs Normal, COVID19 vs Viral pneumonia and COVID19 vs Bacterial pneumonia respectively.

1.1.7 COVIDXnet

E El-Din et al. proposed COVIDXnet architecture, which is a deep learning framework to diagnose COVID19 CXR images. They have compared 7 different models to classify CXRs as COVID19 or non COVID19 [5]. The dataset used is the public dataset provided by Dr. Joseph Cohen and Dr. Adrina Rosebrock, a limited dataset consisting of 50 X-ray images of which 25 normal (health) and 25 positive COVID19 images. They have trained and analyzed VGG!9, DenseNet201, ResNetV2, InceptionV3, Inception-ResNetV2, Xception and MobileNetV2. They have used 80% of the available for training/evaluation and 20% to test and compare the performances. From their study, it was concluded that VGG19 and DenseNet201 models are better/recommended whereas InceptionV3 did not perform well when compared to other deep learning models.

1.1.8 COVID-ResNet

M Farooq and A Hafeez suggested this architecture, COVID-ResNet [3], they have used ResNet50 pre-trained model, applied transfer learning and other hyper-tuning to effectively use it for multiclass classification of CXRs into normal, bacterial, viral and COVID19. With the help of trans-

fer learning techniques they replaced the head of the pre-trained model with another head that contains Adaptive average/max pooling, batch normalization, drop out and linear layers. They then used this model to further stage 2 and stage 3, to hyper-tune the model parameters on different image sizes such as 224X224X3 and 229X229X3 respectively. This architecture achieved overall accuracy of 96.23% compared to COVID-Net with 83.5% on the same COVIDx test dataset. The number of parameters and training epochs are very small compared to COVID-Net architecture.

2. METHOD

The primary objective was to improve the detection of COVID-19 in CXR images with a multi-classifier model that can detect four categories: Normal, Pneumonia Viral, Pneumonia Bacteria and COVID-19. The baseline we will be comparing against is the original FLANNEL architecture. We used the same datasets that were used in the FLANNEL paper, the COVID Chest X-ray Dataset [2] from GitHub and the Kaggle Chest X-ray images dataset. Similar to the FLANNEL paper, we also restricted the types of images used to anteroposterior (AP) or posteroanterior (PA). The restricted images were then labelled appropriately into one of the four categories.

2.1 Segmentation Training

The first major data pre-processing step that we performed on our dataset was segmentation. In order to accomplish this, we recreated the same segmentation network that Park et al. used for their patch-based classification; FC-DenseNet103 [6]. We trained the FC-DenseNet103 model using PyTorch to produce a mask of the lung contours of a CXR image. The datasets that were used to train the segmentation network were the Japanese Society of Radiological Technology (JSRT) dataset which contained 247 PA CXR images and the Segmentation in Chest Radiographs (SCR) database which contains segmentation masks for the CXR images from the JSRT dataset. The JSRT/SCR dataset were ran-

Table 1: Experimental data description

| Source | | Total | COVID-19 | Viral | Bacterial | Normal |
|----------------------|----------|-------|----------|-------|-----------|--------|
| Old data | CCX data | 119 | 100 | 11 | 7 | 1 |
| | KCX data | 5389 | 0 | 1492 | 2780 | 1117 |
| Current data | CCX data | 554 | 478 | 16 | 42 | 18 |
| | KCX data | 5856 | 0 | 1493 | 2780 | 1583 |
| View Distribution | AP view | 6163 | 282 | 1501 | 2789 | 1591 |
| | PA view | 247 | 196 | 8 | 33 | 10 |
| Training/test splits | Training | 5127 | 378 | 1509 | 2291 | 1288 |
| | Testing | 1283 | 100 | 339 | 531 | 313 |
| | Total | 6410 | 478 | 1509 | 2822 | 1601 |

AP: anteroposterior; CCX: COVID Chest X-ray; COVID-19: coronavirus disease 2019; KCX: Kaggle Chest X-ray; PA: posteroanterior.

domly split where 80% of images were used for training and 20% were used for validation; this resulted in 197 images being used for training and 50 images being used for validation for the JSRT dataset as shown in Table 2. Since CXR images from different data sources will come in a wide variety of formats, the JSRT dataset was pre-processed by performing data type casting to float32, histogram equalization to adjust the contrast, gamma correction to adjust brightness and standardizing the image size by resizing it to 256x256. During training, the network parameters were initialized with a random distribution and the Adam optimizer was used with an initial learning rate of 0.0001. The learning rate was decreased by a factor of 10 when there was no improvement in the loss. The Jaccard Index (JI) was used to evaluate the model during training since we were comparing the similarity of the mask produced by the network to the mask provided in the SCR dataset. An early stopping strategy was used based on the validation performance to prevent the model from overfitting.

We then applied the trained FC-DenseNet103 segmentation model on the AP and PA CXR images from the COVID Chest X-ray and Kaggle X-ray datasets. These datasets now contains 478 COVID-19 and 5932 non-COVID CXR images. The original inference script provided by Park et al. would produce two outputs, a Numpy¹ format from the CXR and a Numpy format of the mask separating the lung contours. The Numpy format of the mask is just 0s and 1s where the 1s represent the area of the lung contours. We modified the inference script to apply the mask to the CXR by performing together by performing multiplication, we then saved the Numpy compressed version of the masked CXR. This modification has two benefits, the first being that less disk space is used and the second being that our dataloader for the patch-based classifiers can improve performance since they no longer have to be responsible for applying the mask to the CXR as which was done by Park et al. We then split the masked CXR dataset using a train-test ratio of 4:1 to randomly generate train test splits. To ensure reporting accurate performance on the base models, we used five fold cross validation while training. The detailed statistics are shown in Table 1. In the same table, we also present statistics for old data that was used in FLANNEL paper [10] to show the improved distribution of COVID-19 images.

¹<https://numpy.org/devdocs/reference/generated/numpy.lib.format.html>

2.2 Base model training

The next improvement that we produced was creating patch-based classifiers. Similar to the original global base models in FLANNEL, the patch base models used were pre-trained from ImageNet² to account for the small size of the dataset. The patch-based classifier then produced k number crops/patches of size 224x224 from the masked CXR generated in the previous step. To limit patches outside the lung area, the random points were forced to be within the lungs and the random point was used as the center of the patch. During inference, the k should be large enough to ensure that the lung pixels are covered multiple times. Each patch is then fed into a network to produce a prediction. The confidence score was calculated for each category by calculating the percentage of predictions for each class based on the k patches. The optimization algorithm used during training was the Adam optimizer with a learning rate of 0.00001. An early stopping strategy based on validation performance was applied. The best model is selected among 100 epochs training.

2.3 Ensemble model learning

Ensemble model learning step is similar to baseline FLANNEL paper. We take N base models predictions and concatenate them as f and feed them in neural weight module to learn base model weight.

We calculate outer product ff^t which is flattened and fed into dense neural network with TanH layer to map features into base models weights. Then we train the ensemble model to learn optimal weight combination by feeding linear combination of predictions and weights of base models. The neural weight module uses a modified Focal loss function to handle multiclass classification.

The neural weight module uses a modified Focal loss function to handle multiclass classification. It downweights the well classified classes, in-favor of poorly classified classes so the model can focus on learning imbalanced examples.

$$LossFunc = FocalLoss(\hat{y}, y) \quad (1)$$

$$= \sum_{m=1}^M -\alpha_m y_m (1 - \hat{y}_m)^\gamma \log \hat{y}_m \quad (2)$$

Where $(1 - \hat{y}_m)^\gamma$ is a modulating factor with tunable focusing

²<http://www.image-net.org/challenges/LSVRC/index>

parameters γ and α_m [10]. α_m is set to be inverse class frequency of each class. The overall algorithm is shown in Algorithm 1.

Table 2: FCDenseNet103 Segmentation Training & Validation Dataset

| Dataset | Number of images |
|------------|------------------|
| Training | 197 |
| Validation | 50 |

Algorithm 1: Patched-FLANNEL Training

Input :

X-ray Images, Class Labels

Segmentation Model

Base Models $\{Learner_1, Learner_2, \dots, Learner_n\}$

(Define B as batch size)

(Define K patch count)

Stage 1:

Run segmentation network on the dataset to generate masks for each CXR image.

Stage 2:

For each batch of images and labels **do**

1. Fetch the masked CXR image.
2. Separate image into random k patches.
3. Pass random k -patches to base models.
4. Get mean probability score from all Base Models.
 $P_i = Learner_i(X) \in R^{B \times 4}$, where $i = 1, \dots, n$
5. Get Learner weights.
 $W = NeuralWeightModule([P_i, i = 1, \dots, n]) \in R^{B \times 5}$
6. Linear Combination for Prediction
 $\hat{Y} = Softmax(\sum_{i=1}^n W_i P_i) \in R^{B \times 4}$ (where W_i represents i -th column of W)
7. Loss = $FocalLoss(\hat{Y}, Y)$
8. Back-propagate on Loss and update parameters

End

3. RESULTS

We chose 5 base models for FLANNEL framework: Densenet161, InceptionV3, Resnet152, Resnet101 and Vgg19_bn. These models were fine-tuned using default parameter values, settings and by using the Adam optimizer. We compared FLANNEL with these 5 base models of the framework.

We trained the FC-DenseNET 103 segmentation model successfully and produced masked CXR images that only display the lung area for the updated FLANNEL dataset. We also created and trained patch-based versions of the original FLANNEL base models that use masked CXR images. We performed the FLANNEL ensemble with the results of the patch-based classifiers and compared the performance with the original FLANNEL architecture.

3.1 Implementation details

Segmentation model (FC-DenseNet103), patched FLANNEL base and ensemble models are implemented in PyTorch. Segmentation model is trained on NVIDIA GTX1080 GPU on a Windows 10 desktop. Rest of the models are trained on AWS p3.2xlarge EC2 (virtual machine) instances featuring NVIDIA Tesla V100 GPUs on Ubuntu 18.04. The base

models are fine tuned using weights from pre-trained models. The data are augmented with random flips, crops and scaling during the fine tuning process.

We created and trained patch-based versions in the same environment as the original FLANNEL base learners. The primary difference was that the dataset fed to the patch-based learners was the masked CXR images. Since the CXR images were already masked, no random flips, crops or scaling was applied to the data for training.

After the base models are trained, the FLANNEL ensemble is trained by passing in the concatenated output layers of the base models as the input features.

3.2 Evaluation strategy

Our main goal is to study the detection of COVID-19 among different respiratory x-ray images. We first measured the overall accuracy and precision of all 4 classes of x-ray images (COVID-19 viral pneumonia, non-COVID-19 viral pneumonia, bacterial pneumonia and normal images).

For each class of image, we record precision and recall values for each fold. We calculate F1-score for each fold and then average them to calculate the mean F1 score.

We evaluate original FLANNEL *global*³ base models independently, the global ensemble model, the patch-based base models independently and the patch-based FLANNEL ensemble model.

3.3 Experimental Results

3.3.1 Segmentation Training

Training the Segmentation Network on the JSRT/SCR dataset had a Jaccard Index (JI) score of 93.39% for creating the lung contour masks. The Figure 2 shows the mask creation and applying the mask on the image.



Figure 2: Segmentation Training

3.3.2 FLANNEL

In this section, we compare original FLANNEL base models and ensemble performance with the patched FLANNEL. Because COVID-19 class is heavily imbalanced compared to other categories, overall accuracy would not be the appropriate measure for performance evaluation. It would not be able to show performance increase in COVID-19 detection, So instead we use F1-score for COVID-19 vs rest comparing the different models. As shown in Figure 3, we can see the ensemble approach in the original FLANNEL clearly outperforms state-of-the-art base models in detecting COVID-19. We however, don't see the same performance gain in the patched FLANNEL approach where ensemble performance is slightly worse than the original FLANNEL model. We see a 1.17% decrease in F1-score compared to original FLANNEL model. We do notice significant improvement in all

³Complete image as input instead of patch

Table 3: Performance comparison on F1 score: Class-specific F1 score is calculated using 1 class vs the rest strategy

| | COVID-19 | Pneumonia virus | Pneumonia bacteria | Normal | Macro-F1 |
|-------------------------|---------------|-----------------|--------------------|---------------|---------------|
| Original FLANNEL | | | | | |
| Densenet161 | 0.7694 (0.03) | 0.5901 (0.05) | 0.8030 (0.01) | 0.8875 (0.02) | 0.7625 (0.02) |
| InceptionV3 | 0.8938 (0.01) | 0.6413 (0.03) | 0.8112 (0.02) | 0.9015 (0.03) | 0.8120 (0.02) |
| Resnet152 | 0.8302 (0.02) | 0.6218 (0.02) | 0.8046 (0.01) | 0.9080 (0.00) | 0.7911 (0.01) |
| ResNeXt101 | 0.8197 (0.03) | 0.6151 (0.04) | 0.8016 (0.01) | 0.9046 (0.01) | 0.7852 (0.02) |
| Vgg19_bn | 0.8753 (0.02) | 0.6023 (0.01) | 0.8016 (0.01) | 0.8950 (0.00) | 0.7936 (0.00) |
| FLANNEL | 0.9239 (0.01) | 0.6675 (0.02) | 0.8306 (0.01) | 0.9322 (0.00) | 0.8385 (0.01) |
| Patched FLANNEL | | | | | |
| Densenet161 | 0.8994 (0.02) | 0.5815 (0.02) | 0.8171 (0.01) | 0.9195 (0.01) | 0.8043 (0.01) |
| InceptionV3 | 0.8974 (0.03) | 0.6161 (0.00) | 0.8286 (0.00) | 0.9351 (0.01) | 0.8193 (0.01) |
| Resnet152 | 0.8738 (0.02) | 0.5527 (0.03) | 0.8204 (0.00) | 0.9133 (0.00) | 0.7901 (0.01) |
| ResNeXt101 | 0.8978 (0.01) | 0.5875 (0.01) | 0.8215 (0.01) | 0.9200 (0.01) | 0.8067 (0.00) |
| Vgg19_bn | 0.8870 (0.03) | 0.5786 (0.03) | 0.8201 (0.00) | 0.9159 (0.01) | 0.8004 (0.01) |
| FLANNEL | 0.9121 (0.02) | 0.6009 (0.01) | 0.8270 (0.01) | 0.9319 (0.01) | 0.8180 (0.01) |
| FLANNEL_OldData | 0.8168 (0.03) | 0.6063 (0.02) | 0.8267 (0.00) | 0.9144 (0.01) | 0.7910 (0.01) |

The values in parentheses are the standard deviations.

patched base models compared to the original base models for COVID-19 detection.

In Table 3, we show F1-score for each classification and macro F1-score for all classes. In Table 3, we can see original FLANNEL performs better than base models and also performs better than FLANNEL run with old dataset[10]. We see 13.11% increase in performance of original FLANNEL when run on new dataset. This can be attributed to now much better distribution of COVID-19 images in current data. In patched based models, we see all base models are performing better than original base models except for Pneumonia virus classification. However, patched FLANNEL performs slightly poor in all four classification. We see a decrease of 2.44% in macro-F1 score for patched FLANNEL compared to original FLANNEL.

We now compare the performance of the original FLANNEL ensemble with the patched FLANNEL ensemble using micro-averaged precision and recall and see a slight increase in overall performance compared to the original approach. This is apparent in comparison of Precision-Recall curves in Figure 6 and ROC (Receiver operating characteristic) curves in Figure 5 of both ensemble method. As shown in Figure 6 We see a 1.15% increase in precision-recall AUC (Area under curve) and 2.08% increase in ROC AUC. As micro-average gives equal weight to all predictions irrespective of classes. This shows patched ensemble model performs slightly better in overall predictions.

We also compare the patched and original FLANNEL performance via confusion matrix as shown in Figure 7 and Figure 8. Due to nature of random split between different runs, we see different numbers in both confusion matrix. However it still provides enough information for us to compare. We see patched and original FLANNEL performs similarly in detection of COVID-19 images where it has higher precision and recall than other two types of Pneumonia. Both models struggle with Pneumonia viral images classification and misclassifies them as Pneumonia bacteria images.

We also present the ROC and Precision-Recall curve for COVID-19 classification in Figure 4 to show diagnostic ability of patched FLANNEL. We noted that ROC curve can be misleading for highly imbalanced classifications. As we

see using ROC curve AUC gives an impression of all models are performing well as they have very few false positives. However when we look at PR curve, we could see models performance differ and InceptionV3 and Ensemble model performing better than others.

4. DISCUSSION

We realized very early in the project that running FLANNEL model using five base models and 200 epochs for five folds is going to take at least 3-4 days on a high end GPU (Tesla V100 GPU or equivalent). We had to find a solution on both cost and runtime in order to have results early. We tried multiple optimization methods such as increasing the number of workers, mounting training images in memory to bring the runtime down. We also used spot instances in parallel to bring the cost down. We were able to faithfully reproduce original FLANNEL and complete patched FLANNEL in a considerable short time with significantly low cost. It took us 36 hours (144 compute hours) for original FLANNEL and 10 hours (800 compute hours) for patched FLANNEL. The whole project costed us around \$300.

Training the original FLANNEL model is already extremely slow as training single model takes on average 2-3 hours. When using the original architecture for the patch-based models, the training process was even slower due to two reasons. The first is that the patch-base model data-loader was originally responsible for applying the mask to the CXR image, this was addressed by transitioning the responsibility to the segmentation task to immediately apply the mask to the CXR. The second reason for the patch-based models being slow is that a classification is run for each patch sequentially. This increases the complexity from N to $k \times N$ where k is the number of patches. We were unable to address this due to time constraints but we believe parallelizing the patch predictions could lead to major improvements.

After training the patch-based models we were hoping to see substantial improvements similar to Park et al. but we only noticed minor changes in performance where some models slightly increased while others decreased. Two models that had an increase in average precision performance were inceptionv3 and densenet161. While resnet152, resnext101 and

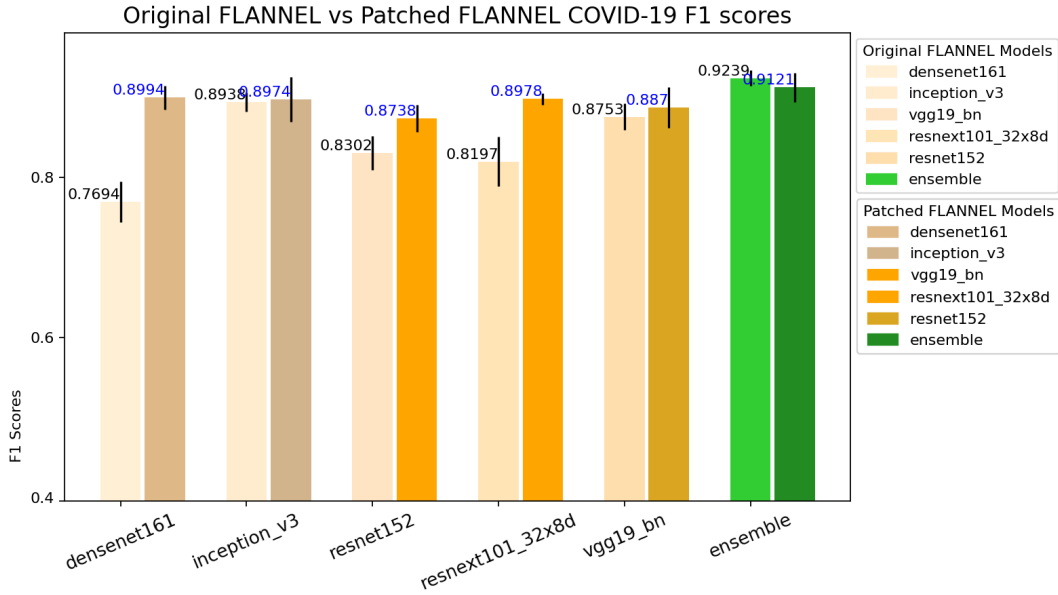


Figure 3: COVID-19 F1 score comparison

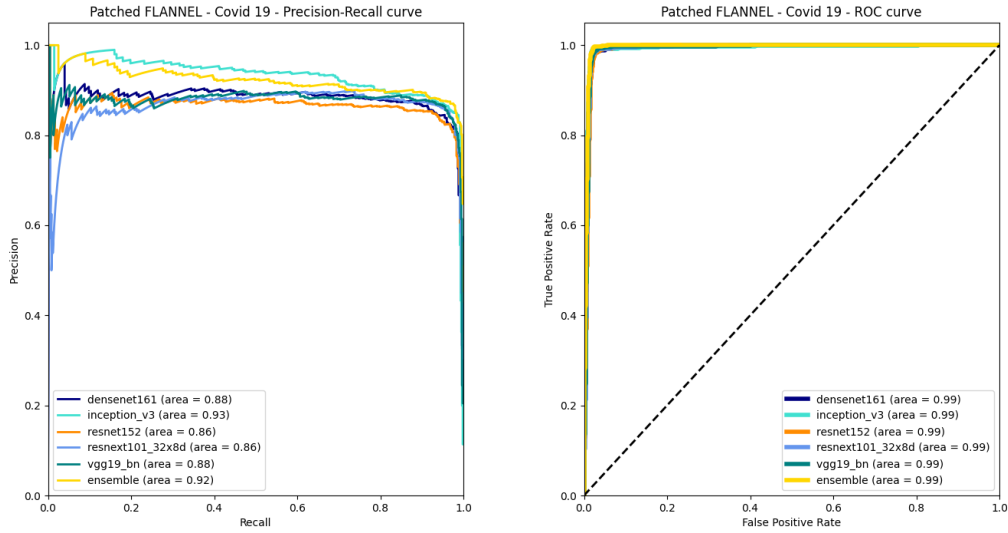


Figure 4: Patched FLANNEL PR and ROC Curve

vgg19_bn had minor decreases in average precision. Even though three of the base-models had decreased performance, the patched ensemble still had a minor improvement over the base ensemble in average precision by 1%. We were originally hopeful to have more significant increases in performance. Some of the reasons that could explain this result is the segmentation that generated the masked CXR is inaccurate and is masking important information surrounding the edges of the lungs. This hypothesis will need to be verified by a medical expert. Another reason the patch-based method was not as effective was that local patterns within the lung areas of a CXR are less important than the global

patterns detected within a lung. This hypothesis can potentially be tested by increasing the patch size and measuring performance again.

Some changes we made that could have decreased the patch-based model performance are removing the weight assignment step from the patch classifier and limiting the training to 100 epochs. The weight assignment step was removed because we thought the probabilities of the classification output were already being passed through an ensemble method where a neural network learns appropriate weights based on class imbalance.

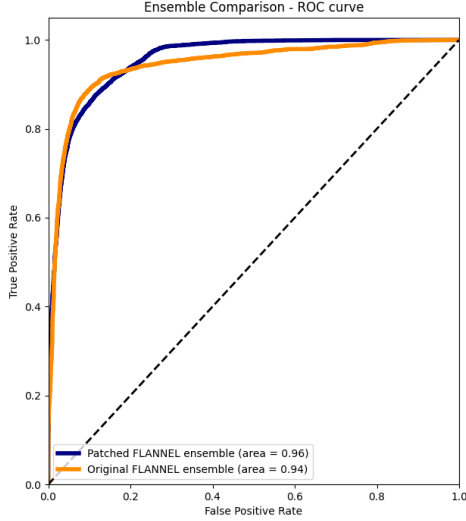


Figure 5: Ensemble Comparison ROC Curve

5. CONCLUSION

We had two major goals for this project. To faithfully reproduce FLANNEL on an updated dataset with improved distribution of COVID-19 images and to apply segmentation and patched classification to improve the COVID-19 detection performance of FLANNEL model.

We ran the base models and FLANNEL ensemble on the new dataset using all five folds and 200 epochs. With the improved distribution of COVID-19 data we see FLANNEL outperforms the metrics as seen in the original FLANNEL paper by 13%. This large increase in performance highlights the importance of curating a rich dataset.

Then we created the Segmentation model that produced masked CXR images that displayed only the lung contours. These masked images were then used as a dataset for patch-based versions of the FLANNEL model. The performance of the patch-based models based on F1-Score had significant improvements when compared with their original counterparts with the exception of the Pneumonia Viral class. We then ran the ensemble on the outputs of the patch-based classifier and did not note major improvement in classification performance. For COVID-19, ensemble on patched classifiers performed slightly worse than Original FLANNEL ensemble. However, for overall classification the average precision increased by 1% over the Original FLANNEL.

We trained patched base models for 100 epochs as done in the patch classification paper and patched FLANNEL ensemble for 200 epochs.

We were partially able to achieve our goal of improving the original FLANNEL architecture using patch-based models. Even though the performance was slightly increased, we see both Original FLANNEL and Patched FLANNEL clearly outperforms the other base models.

6. CONTRIBUTION

All authors were actively involved in Patched FLANNEL development and implementation. Major contributions from

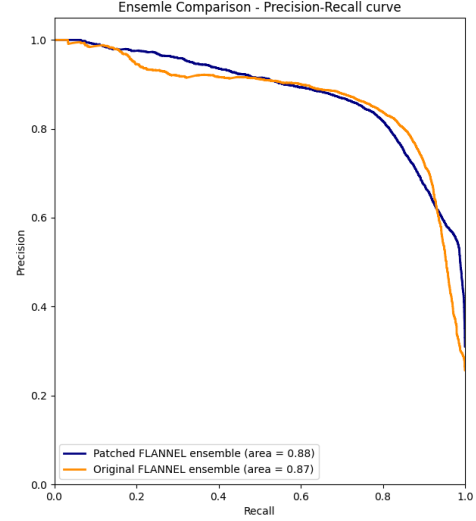


Figure 6: Ensemble Comparison PR Curve

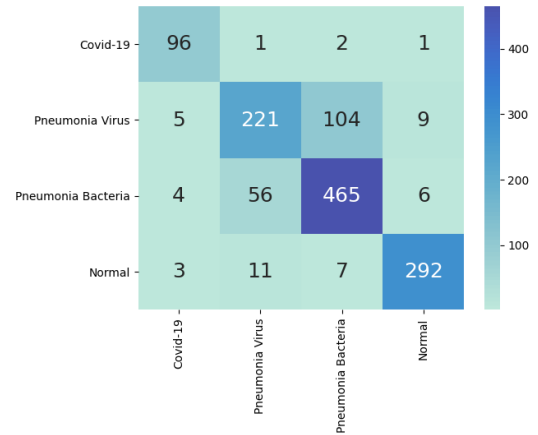


Figure 7: Original FLANNEL Confusion Matrix

authors are:

Maneesh: AWS Setup, batch run of FLANNEL and patch-based models on AWS, patch-based classification and ensemble model development, project report, GitHub documentation

Raman: segmentation and patch-based classification development, output graphs, presentation slide, project report, GitHub documentation

Satish: FLANNEL checkpoints, output graphs and reports development, GitHub documentation, presentation video

Srikanth: segmentation, patch-based classification development, project report, GitHub documentation, presentation video

7. ACKNOWLEDGEMENT

GitHub source code for both FLANNEL and Patch-Based classification [9] paper are used as baseline for this improvement.



Figure 8: Patched FLANNEL Confusion Matrix

- FLANNEL GitHub Repository
- Patch-Based classification

8. APPENDIX

GitHub source code for the Patched FLANNEL <https://github.com/mannbiher/DeepLearningForHealthCareProject>

9. REFERENCES

- [1] H. X. Bai, R. Wang, Z. Xiong, B. Hsieh, K. Chang, K. Halsey, T. M. L. Tran, J. W. Choi, D. C. Wang, L. B. Shi, J. Mei, X. L. Jiang, I. Pan, Q. H. Zeng, P. F. Hu, Y. H. Li, F. X. Fu, R. Y. Huang, R. Sebro, Q. Z. Yu, M. K. Atalay, and W. H. Liao. Artificial Intelligence Augmentation of Radiologist Performance in Distinguishing COVID-19 from Pneumonia of Other Origin at Chest CT. *Radiology*, 296(3):E156–E165, 09 2020.
- [2] J. P. Cohen, P. Morrison, L. Dao, K. Roth, T. Q. Duong, and M. Ghassemi. Covid-19 image data collection: Prospective predictions are the future. *arXiv 2006.11988*, 2020.
- [3] M. Farooq and A. Hafeez. Covid-resnet: A deep learning framework for screening of covid19 from radiographs, 2020.
- [4] L. K. Hansen and P. Salamon. Neural network ensembles. *IEEE Transactions on Pattern Analysis and Machine Intelligence*, 12(10):993–1001, 1990.
- [5] E. E.-D. Hemdan, M. A. Shouman, and M. E. Karar. Covidx-net: A framework of deep learning classifiers to diagnose covid-19 in x-ray images, 2020.
- [6] S. Jégou, M. Drozdal, D. Vázquez, A. Romero, and Y. Bengio. The one hundred layers tiramisu: Fully convolutional densenets for semantic segmentation. *CoRR*, abs/1611.09326, 2016.
- [7] T.-Y. Lin, P. Goyal, R. Girshick, K. He, and P. Dollár. Focal loss for dense object detection, 2018.
- [8] A. Narin, C. Kaya, and Z. Pamuk. Automatic detection of coronavirus disease (covid-19) using x-ray images and deep convolutional neural networks. *Pattern Analysis and Applications*, May 2021.
- [9] Y. Oh, S. Park, and J. C. Ye. Deep Learning COVID-19 Features on CXR Using Limited Training Data Sets. *IEEE Trans Med Imaging*, 39(8):2688–2700, 08 2020.
- [10] Z. Qiao, A. Bae, L. M. Glass, C. Xiao, and J. Sun. FLANNEL (Focal Loss bAsed Neural Network Ensemble) for COVID-19 detection. *Journal of the American Medical Informatics Association*, 28(3):444–452, 10 2020.
- [11] A. Sharkey. On combining artificial neural nets. *Connect. Sci.*, 8:299–314, 12 1996.
- [12] G. Wang, X. Liu, C. Li, Z. Xu, J. Ruan, H. Zhu, T. Meng, K. Li, N. Huang, and S. Zhang. A Noise-Robust Framework for Automatic Segmentation of COVID-19 Pneumonia Lesions From CT Images. *IEEE Trans Med Imaging*, 39(8):2653–2663, 08 2020.
- [13] L. Wang and A. Wong. Covid-net: A tailored deep convolutional neural network design for detection of covid-19 cases from chest x-ray images, 2020.
- [14] WHO Emergency Response Team. Weekly epidemiological update on covid-19 - 20 april 2021. Technical report, WHO, April 2021.